Two-photon absorption cross section measurements of various two-photon initiators for ultrashort laser radiation applying the Z-scan technique

A. Ajami,[1,*] W. Husinsky,[1] R. Liska,[2] and N. Pucher[2]

[1]*Vienna University of Technology, Institute of Applied Physics, Wiedner Hauptstrasse 8-10, 1040 Wien, Austria*
[2]*Vienna University of Technology, Institute of Applied Synthetic Chemistry, Getreidemarkt 9, 1060 Wien, Austria*
**Corresponding author: Ajami@iap.tuwien.ac.at*

Received July 28, 2010; revised September 7, 2010; accepted September 9, 2010; posted September 10, 2010 (Doc. ID 132470); published October 14, 2010

In this paper, we describe the Z-scan measurements of the two-photon absorption (TPA) cross section of various two-photon initiators that are suitable for real three-dimensional structuring of photo-polymerizable formulation. The value of the TPA cross section for the initiator P3K was measured to be 256 GM as the maximum value among the synthesized initiators. Procedures for a precise Z-scan measurement including the measurement of Rayleigh length and beam waist radius are presented. The effect of the pulse width on the Z-scan signal is demonstrated. We also used a flow-cell geometry instead of a static cell in order to refresh the materials to avoid the decomposition of the molecules. This resulted in a more realistic TPA cross section which has been proven by suitable reference compounds. © 2010 Optical Society of America

OCIS codes: 190.4180, 190.4710, 160.4330, 120.6710.

1. INTRODUCTION

The observation that the absorption coefficient of materials can increase or decrease with intensity is referred to as nonlinear absorption, which is frequently observed in many materials exposed to ultrashort laser pulses. The former (increase) is called reverse saturable absorption and can be caused by multi-photon absorption (MPA) [two-photon absorption (TPA) or three-photon absorption] or excited state absorption (ESA). The latter (decrease) is known as saturable absorption (saturation of the linear absorption) [1]. In the case where the absorption coefficient increases with intensity, it is a serious challenge to determine which kind of absorption takes place for a typical material under investigation. TPA is a third-order nonlinear resonance process, where two photons are simultaneously absorbed to excite the subject molecule from ground state to a real exited state through an intermediate virtual state [2]. In the simultaneous presence of ESA and MPA it is difficult to measure pure MPA coefficients, because in many cases the experimental technique cannot distinguish between the individual nonlinearities [3]. The advantage of using low repetition rate laser pulses is that the ESA does not contribute significantly to nonlinear absorption.

TPA in molecular systems using near infrared ultrashort pulsed laser radiation has attracted much attention of researchers due to its potential applicability in the field of modern photonics such as two-photon induced photo-polymerization (TPIP) [4], three-dimensional (3D) optical data storage [5], photonic crystals [6], photodynamic therapy [7], two-photon fluorescence microscopy [8], and many more. This wide range of applications of TPA has encouraged many researchers to put much emphasis on designing and synthesizing organic molecules with significantly higher TPA cross sections than in common materials [9].

Several different experimental techniques can be employed to measure TPA cross sections such as nonlinear transmission [10], upconverted fluorescence emission [11], transient absorption [12], four-wave mixing [13], and the Z-scan technique [14]. Among these techniques, the Z-scan technique, which was first introduced by Sheik-Bahae *et al.* in 1990 [15], is a particularly sensitive technique [16] and is very easy to perform. It is especially suitable for non-fluorescence materials, for which the upconverted fluorescence emission experiment is not an appropriate method to measure TPA cross sections. This technique relies on the transformation of phase distortion to amplitude distortion during beam propagation through a nonlinear medium. Z-scan can be performed in two ways. The open-aperture (OA) Z-scan method, which is sensitive to nonlinear absorption, and the closed-aperture (CA) Z-scan version, which is sensitive to nonlinear absorption as well as the nonlinear refractive index.

Modifications of the original Z-scan technique have been proposed, such as the two-color Z-scan [17] [to measure the non-degenerate susceptibility at frequencies ω (probe beam frequency) and ω_p (pump beam frequency)], the eclipse Z-scan [18] (the aperture in the CA Z-scan is replaced with an obscuration disk with a diameter smaller than the beam size), the reflection Z-scan method [19] (the reflected laser beam from a non-transparent ma-

terial is monitored through an aperture), the second Z-scan [20] (provides measurement of the nonlinear absorption and the nonlinear refraction in the materials for which the nonlinear refraction is accompanied by the nonlinear absorption performing OA and CA Z-scans separately at the same conditions), off-axis Z-scan [21] (the aperture placed on the optical axis for on-axis Z-scan is transversely shifted), and the so-called differential Z-scan technique [22] [in which the sample oscillates along the optical axis on each position, and the differential transmission (not total intensity transmission) is measured as a function of the sample position]. In essence, in an OA Z-scan experiment, a nonlinear medium is translated along the beam propagation direction through the focus of a tight focused laser beam, and the laser energy transmitted through the sample is measured as a function of the sample position. By fitting the theoretical curve to the experimental data [16], the nonlinear absorption coefficient could be extracted when the Rayleigh length, the beam waist radius, and the peak intensity at the focus are known.

To determine a reliable TPA cross section, a few requirements have to be fulfilled such as a stable laser system, a well aligned Z-scan setup, and a practicable method to determine the beam waist radius and the Rayleigh length. In this paper the TPA cross section for a series of two-photon initiators (TPIs) for TPIP has been investigated using the OA Z-scan technique [23]. We propose what we believe to be a new method to measure the beam waist radius by scanning an aperture along the beam propagation direction. We also explain how the beam quality factor M^2 must be taken into account. This might be the reason why different TPA cross sections for various reference dyes such as Rhodamine B have been reported in the literature [24]. The effect of the pulse duration on the OA Z-scan signal will also be discussed, and furthermore it will be demonstrated that refreshing materials results in measuring a more realistic TPA cross section.

2. THEORETICAL CONSIDERATIONS

For a molecular system, the TPA cross section σ describes the efficiency of a particular molecule in the ground state to reach the excited state via a TPA process, and it is defined as follows:

$$\sigma = \frac{\hbar\omega\beta}{N_A\rho \times 10^{-3}}(\mathrm{cm}^4\ \mathrm{s\ photon}^{-1}\ \mathrm{molecule}^{-1}), \quad (1)$$

where $\hbar$ is the reduced Planck constant, N_A is Avogadro's number, and ρ is the concentration in mole per liter [25]. σ is commonly given in a new SI unit (GM) defined as $1\ \mathrm{GM} = 10^{-50}\ \mathrm{cm}^4\ \mathrm{s\ photon}^{-1}\ \mathrm{molecule}^{-1}$.

The normalized transmittance through a nonlinear medium where TPA occurs is given by [16]

$$T(z) = \sum_{n=0}^{\infty} \frac{(-q_0)^n}{(n+1)^{3/2}(1+x^2)^n}, \quad (2)$$

where $x = z/z_R$, $q_0 = \beta L_{\mathrm{eff}} I_0$, $L_{\mathrm{eff}} = (1 - e^{-\alpha_0 L})/\alpha_0$, and I_0 is the maximum on-axis intensity in the focus. The TPA coefficient β can be extracted by fitting to the experimental data using Eq. (2) provided that I_0 and z_R have already been measured. The TPA cross section is also obtained from Eq. (1) for any solution with a certain concentration.

Assuming a Gaussian pulse form, I_0 can be calculated from the following relation:

$$I_0 = 4\sqrt{\frac{\ln 2}{\pi}}\frac{P_{\mathrm{Aver}}}{\pi\omega_0^2 R\tau} = 4\sqrt{\frac{\ln 2}{\pi}}\frac{P_{\mathrm{Aver}}}{M^2\lambda z_R R\tau}, \quad (3)$$

where P_{Aver} is the average laser power, ω_0 is the beam waist radius, R is the pulse repetition rate, τ is the pulse width, z_R is the Rayleigh length, and M^2 is the beam quality factor. The power $P(z,t)$ transmitted through an aperture of radius a located at the position z is given by

$$P(z,t) = \frac{\pi\omega_0^2}{2} I_0(z,t)(1 - e^{-2a^2/\omega(z)^2}), \quad (4)$$

where a is the aperture radius, and $\omega(z)$ is the beam radius in the aperture plane given as

$$\omega(z)^2 = \omega_0^2\left(1 + \frac{z^2}{z_R^2}\right). \quad (5)$$

Therefore, the normalized aperture transmittance as a measurable quantity is defined as the quotient of the aperture transmittance at the position z to the transmittance at the beam waist position:

$$T_{\mathrm{Norm}}(z) = \frac{1 - e^{-2a^2/\omega(z)^2}}{1 - e^{-2a^2/\omega_0^2}}. \quad (6)$$

If one scans an aperture along the laser beam propagation direction and measures the energy transmitted through the aperture as a function of the aperture position relative to the focus, the beam waist radius can be obtained by means of the theoretical fitting to the measured data using Eq. (6) provided that the Rayleigh length has been measured via other means. By using a beam profiler for measuring the beam diameter at different positions within the vicinity of focal point and also at far enough from the focus and then fitting to the measured data using Eq. (5), one could obtain the Rayleigh length.

3. EXPERIMENTS

A. Sample Preparation

The fluorescence dye standards (Rhodamine B and Rhodamine 6G) were bought from Sigma-Aldrich and used as received. Detailed information on the syntheses, spectroscopic data, and TPIP activity of the TPIs (H3K, O3K, M3K, M2K, B3K, P3K, M3P, M3P+, R1, and R2) could be found elsewhere [23,26].

For the OA Z-scan measurements an equimolar concentration of the compounds (1×10^{-2} M) was prepared using spectroscopic grade solvents. For the two rhodamine compounds, methanol (MeOH) was chosen as the solvent as often described in the literature in order to achieve a reliable reference and to test the Z-scan device. The other initiators were all dissolved in tetrahydrofuran (THF) as all compounds showed a sufficient solubility in this solvent. For comparison, it is important that the same sol-

vent is used for all compounds, because a different polarity of the solvent causes a change in activity of the molecules.

B. Z-Scan Experimental Setup

We used an ultrashort laser system (FEMTOPOWER Compact PRO). This system delivers ultrashort laser pulses with a maximum average power of approximately 800 mW (800 μJ per pulse) at a repetition rate of 1 kHz. The minimum pulse duration, estimated as the full width at half-maximum (FWHM) of a Gaussian temporal profile, is typically 25 fs and can be stretched up to a few hundreds of femtoseconds with help of a Dazzler system (an acousto-optic programmable dispersive filter) which enables one to control separately both the spectral amplitude and the spectral phase. An autocorrelator (model ENV40CSG from Femtolasers Company) is employed to measure the pulse duration. The bandwidth, estimated as the FWHM of the spectrum profile, is 41 nm and the spectrum is centered at 796 nm. The incident laser power was measured using a digital power meter prior to each measurement before the sample.

The schematic of the experimental setup is shown in Fig. 1. A telescope consisting of a 150 mm focal length convex lens followed by a 100 mm focal length concave lens is used to reduce the beam diameter by a factor of 2/3. This results in a Rayleigh length increased by a factor of 2.25 $=(3/2)^2$ to ensure that it is larger than the thickness of the sample, and thus the criterion of the thin sample is fulfilled for the Z-scan measurements. A continuous variable attenuator (Model C-VARM from COHERENT Company) with a maximum attenuation by a factor of 10^{-7} and a fine pitch adjustment control to precisely set the attenuation is employed to attenuate the pulse energy from several hundred microjoules to a few nanojoules so that an appropriate Z-scan signal with the normalized transmittance higher than 0.765 (corresponds to $q_0<1$) can be achieved.

The transited laser beam through the attenuator is split in two orthogonal directions using a beam splitter (67% transmission and 33% reflection). The lower intensity part is used as the intensity reference (detected at the reference diode D_r), and the other is directed to the focusing lens (a 175 mm focal length plano–convex lens) and then through the sample. A 0.2 mm thick one-time flow-cell (170.700 QS from HELLMA Company) connected to a syringe pump (NE-300 from SYRINGPUMP) for variable flow rates is used for the test solutions. The flow-cell combined with an *xyz* stage (Newport, M-DS25-XYZ) for fine adjustment of the sample position was mounted on a translation stage (DC-Motor model MFA-CC from Newport Company) and can be moved 25 mm along the beam propagation direction through the beam focus in minimum steps of 50 nm. This allows detecting any small change in nonlinear absorption although, in general, there is no need to translate the sample in steps smaller than 100 μm, because smaller steps lead to a small change in transmittance which is comparable to the experimental errors and thus very difficult to detect. The transmitted energy was collected by a large diameter short focal length lens (50 mm diameter and 60 mm focal length) to ensure that the whole energy transmitted through the sample is collected. A Si diode with a 1 cm^2 detector area was used to measure the transmitted energy. For adjusting the absolute intensity at the diodes, but to stay within their dynamic range, neutral density filters were used. A low-pass filter was mounted before diode D_c, which blocks unwanted emissions such as upconverted fluorescence from the excited sample. The signals at the diodes were recorded with a two-channel personal computer oscilloscope (model Picoscope3204 from Picotech Company). The computer software analyzed the intensity of individual laser pulses (including averaging over several laser shots) and also handled the movement of the translation stage as well as the entire data acquisition process (LabView).

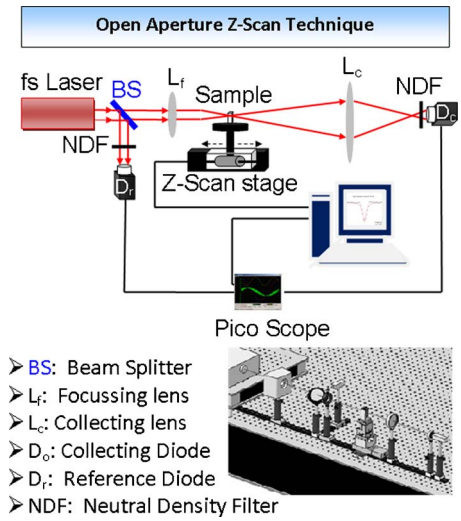

Fig. 1. (Color online) Schematic of the OA Z-scan setup.

C. Rayleigh Length and Beam Quality Measurement

To measure the beam quality factor M^2, we used a beam profiler (model Lasercam HR from Coherent). For this purpose, the camera was mounted in the Z-scan apparatus on the translation stage and was moved along the beam propagation direction in small steps of 0.1 mm. In each position, the laser beam radius was recorded, and the resulting data were fitted to Eq. (5) to obtain the Rayleigh length. The beam waist radius for an ideal Gaussian beam can be calculated from $\omega_0=(\lambda z_R/\pi)^{1/2}$, and then the beam quality factor M^2 can be calculated from $M^2=W_0^2/\omega_0^2$ (W_0 is the measured beam waist radius). After determining the beam quality factor M^2, one can simply replace the wavelength λ with $M^2\lambda$ in all equations [27].

D. Determining the Beam Waist Radius Using the OA Z-Scan Technique

In the previous section, we explained how the Rayleigh length could be determined by measuring the beam radius using a beam profiler. The beam waist radius is predicted within the range of a few tens of micrometers, and hence the value measured by a beam profiler at the focus is not reliable enough because of its limited resolution.

In order to obtain the beam waist radius with the required accuracy, the new method was used. A 50 μm radius aperture was mounted on the translation stage of the Z-scan device. The aperture was moved 10 mm along the

beam propagation direction through the focal point in very small steps of 0.2 mm. The energy transmitted through the aperture was collected with a 60 mm focal length convex lens and detected on diode D_c. The obtained z-dependent transmittance was fitted to Eq. (6) to obtain the accurate beam waist radius as shown in Fig. 3(b) below.

E. Determining the Beam Radius on the Focusing Lens

In most cases found in the literature, the beam waist radius and subsequently the Rayleigh length are calculated from $\omega_0 = \lambda f/\pi\omega$, where f is the focal length of the focusing lens, and ω is the beam radius on the lens. In reality, however, the measured beam waist radius is always larger than the value obtained from the equation above due to the fact that the beam quality factor is larger than 1, even for lasers beams with a TEM_{00} mode. Since, according to the equation above, any inaccuracy in ω results in an equal error for ω_0, and consequently for the TPA cross section, the beam diameter on the focusing lens must be accurately determined. For this purpose, the translation stage was turned by 90°, and a 1 mm diameter aperture was mounted on it so that the plane of aperture was normal to the beam propagation direction. The aperture was scanned orthogonally to the beam propagation direction in steps of 0.4 mm, and the transmitted energy was measured as a function of the aperture position using a photodiode. A Gaussian function was fitted to the measured intensity spatial profile to obtain the beam radius. It is important to show that the measured beam waist radius is equal to the calculated value, if the real beam quality factor $\neq 1$ is taken into account.

4. RESULTS AND DISCUSSION

A. Determining the Beam Parameters

Using the beam profiler [Figs. 2(b) and 2(c)] and the orthogonal scanning method [scanning a 1 mm diameter aperture in the X direction orthogonal to the beam propagation direction; Fig. 2(a)], it could be verified that the intensity profile of the laser beam after the amplifier has a Gaussian spatial profile; therefore, the beam diameter can be determined. From the Gaussian fit to the experimental data in Fig. 2(a) as well as from the two-dimensional (2D) intensity profile measurement using a beam profiler shown in Fig. 2(b), the same beam diameter of 10 mm was obtained (full width at $1/e^2$ of maximum) before the focusing lens.

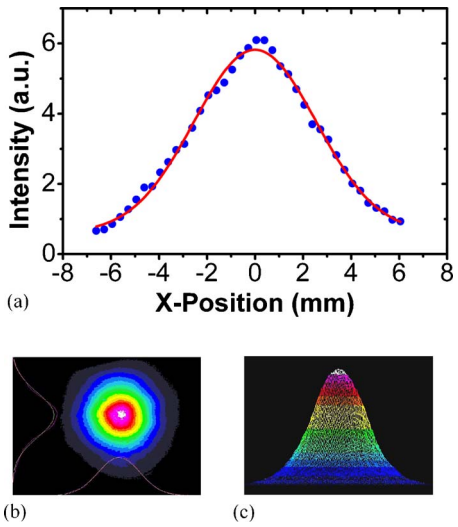

Fig. 2. (Color online) Intensity spatial profile. (a) Transmission through a pinhole scanned orthogonal to the beam propagation direction (scattered points are the experimental data, and the solid line is the Gaussian fit to the experimental data). (b) 2D intensity profile. (c) 3D intensity profile. [Both (b) and (c) were taken by a beam profiler.]

According to the equations mentioned earlier ($\omega_0 = \lambda f/\pi\omega$), with $\omega = 5$ mm, $\lambda = 796$ nm, and $f = 175$ mm, the calculated beam waist radius is 8.9 μm, and consequently a Rayleigh length of 0.3 mm would result. These values are not in agreement with the measured values obtained from the fits to the measured data as shown in Figs. 3(a) and 3(b).

Figure 3(a) shows the beam radius measurement performed using a beam profiler. According to the International Organization for Standardization (ISO) Standard 11146, some data points near the focus and some at a sufficient distance from it are required. Although the beam waist radius measured with the beam profiler is not reliable enough, however, it can be used to obtain the Rayleigh length, because the Rayleigh length is defined as the distance from the focus where the beam radius increases by a factor of $\sqrt{2}$. By fitting to the data in Fig. 3(a) using Eq. (5), a Rayleigh length of 0.7 mm was obtained. As will be shown later, this value for the Rayleigh length resulted in the best fits of the Z-scan data to Eq. (2) for all measurements. This can be taken as a strong argument for the reliability of the Rayleigh length measurement.

Figure 3(b) shows the energy transmitted through an aperture (50 μm diameter) scanned along the beam

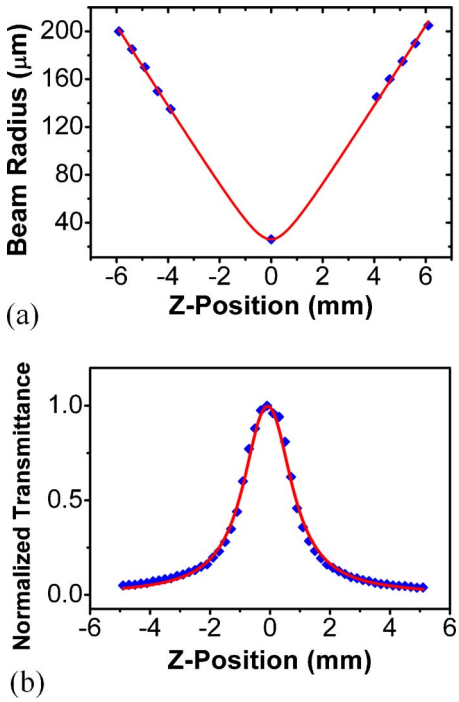

Fig. 3. (Color online) (a) Beam radius versus the z position measured from the focal point. (b) Normalized transmittance through a 50 μm diameter aperture versus the aperture position measured from the focal point.

Table 1. Beam Waist Radius Obtained by Different Methods

ω_0 (μm)	Method
8.9	Calculated from $\omega_0=\lambda f/\pi\omega$ ($f=175$ mm and $\omega=5$ mm)
13.35	Calculated from $\omega_0=(\lambda z_R/\pi)^{1/2}$ ($z_R=0.7$ mm)
20	Obtained from fit to the data using Eq. (6) in Fig. 3(b)
20	Calculated from $\omega_0=M^2\lambda f/\pi\omega$ [$M^2=(20/13.35)^2=2.24$]

propagation direction. Points represent the measured data, and the solid curve is the best fit to the data using Eq. (6) with $z_R=0.7$ mm. A beam waist radius of 20 μm was extracted from the best fit to the data.

The measured beam waist radius W_0 is 20 μm, whereas for an ideal Gaussian beam, a beam waist radius ω_0 of 13.35 μm was calculated (assuming $z_R=0.7$). As a consequence, a beam quality factor M^2 of 2.24 would result. Therefore, one can still use the theoretical Gaussian beam parameters replacing λ with $M^2\lambda$.

In summary, in order to evaluate the TPA cross section in the next section, the beam waist radius values obtained and described above have to be used. See also Table 1 for an ideal and real Gaussian beam.

The value in the first row is invalid for a diffraction-limited beam as well as for a real beam. The value in the second row has been calculated from a Gaussian equation, and it is valid for a diffraction-limited beam. The value in the third row is the experimentally obtained value for the beam waist radius [from fit to the data using Eq. (6) in Fig. 3(b)], and it is valid for the real beam. The value in the fourth row is the calculated value for the beam waist radius from a frequently used equation in the literature ($\omega_0=\lambda f/\pi\omega$), replacing λ with $M^2\lambda$ in order to take into account the beam quality factor. It was illustrated that the value theoretically calculated for the beam waist radius is equal to the value experimentally obtained when the beam quality factor is taken into account.

B. TPA Cross Sections

All the following measurements for the determining of the TPA cross section have been performed with 100 fs pulses (the pulse width was measured using an autocorrelator after stretching the pulses from 25 to 100 fs using a Dazzler unit). The main reason is that in this case, the results for the standards can be compared to the values from the literature, which is mostly available only for 100 fs pulses. Another important reason is that for shorter pulses (i.e., 25 fs) saturation of the TPA has been observed as shown in Fig. 4. Even though short pulses might be very interesting for many applications, to our knowledge, no theoretical (analytical) model to include saturation is currently available. This will be the subject of later investigations. As an example to demonstrate the difference between Z-scan signals resulted from 25 and 100 fs pulses, we performed Z-scans with 25 and 100 fs pulses having the same energy for Rhodamine B. The observed behavior in the case of 25 fs pulses shows new features. The peak

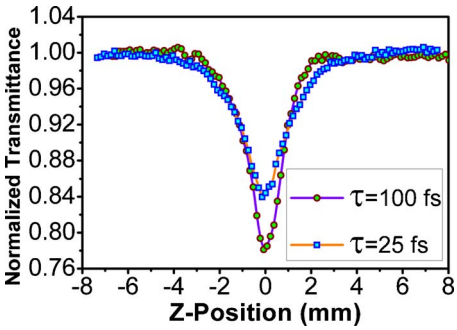

Fig. 4. (Color online) Z-scans for Rhodamine B carried out with the same pulse energy but different pulse widths. Circle points represent experimental data obtained with 100 fs pulses, and square points represent experimental data obtained with 25 fs pulses.

intensity of a 25 fs pulse is four times larger than that of a 100 fs pulse (for the same pulse energy). Since the TPA is proportional to the intensity square, one expects an increase in the absorption with increasing the laser intensity. As seen in Fig. 4, far from the focus where the intensity is quite low, the behavior of the absorption curve is consistent with our expectation, and the absorbance of the 25 fs pulses is larger than that of the 100 fs pulses. But as the sample is moved toward the focus, the absorption of the 25 fs pulses saturates and even decreases with respect to the 100 fs pulses. This unexpected behavior might be caused by saturation and other effects. Investigations are ongoing.

Figure 5 shows the Z-scan for P3K performed with the same pulse energy of 220 nJ, but for different flow rates. As one can clearly observe in Fig. 5, the absorption in case the material is kept flowing through the laser beam is almost twice the absorption without flow. The reason for this is photo-degradation. This can be easily ascribed to the photochemical processes which form the active species for polymerization and which have also a significantly different absorption behavior. Forming the active species during the TPA cross section measurement leads to a decrease in the concentration of initiators. This decrease would reduce the reliability of the TPA measurements as it is based on several individual measurements extended over a certain period with the simultaneous reduction in the number of initiators. Therefore, during the whole TPA measurement always the same concentration should be present, and this can be achieved by a continuous material flow. During photo-polymerization a decrease in the

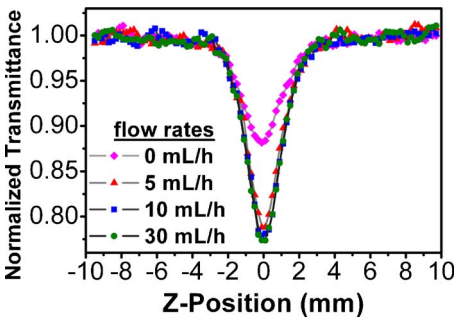

Fig. 5. (Color online) Z-scans for P3K with the same 220 nJ pulses but for different flow rates (without any flow and with 5, 10, and 30 ml/h flow rates).

absorption always occurs as photo-initiating species are formed, which is described as an indicator for an effective TPI.

This phenomenon was also described by Belfield *et al.* [28]. Experimental tests showed that 5 ml/h is the optimum flow rate to refresh the irradiated sample in the focal volume in a reasonable time without losing too much compound; therefore all the following measurements for determining the TPA cross section have been carried out with a 5 ml/h flow rate. In the literature performing the Z-scan itself for different flow rates seems to be more sensitive, and in many cases ultraviolet-visible spectra before and after the exposure are reported to address this issue.

Z-scans for B3K performed at different pulse energies from 30 nJ (corresponds to a peak intensity of 1.01×10^{11} W cm^{-2}) up to 220 nJ are compared in Fig. 6. The relative absorption is linear with the laser intensity, which indicates that the TPA is the predominant nonlinear absorption.

We carried out the same experiments for all samples, but each in an appropriate range of energy. We started performing Z-scan from low energies at which no nonlinear absorption occurs and increased the pulse energy for absorption to appear. We continued to increase the pulse energy up to the value at which the normalized transmittance is reached to 0.765 (which is an indicative of $q_o=1$) or the solvent is started to nonlinearly absorb.

For each sample, we carried out several Z-scans at different pulse energies. Unlike the conventional local fitting, which separately treats data at each pulse energy, we used global fitting for processing Z-scan data which can process a set of experimental data measured with different pulse energies together [29].

In Fig. 7 the results for q_0 versus pulse energy are summarized for all samples. The plots show a linear behavior, which is a clear indication for pure TPA and nonexistence of ESA or any higher order absorption. By fitting to the experimental data using the linear equation $q_0=\beta L_{\text{eff}} I$, where $L_{\text{eff}}=0.2$ mm and I_0 is obtained from Eq. (3), we extracted the TPA coefficients and then calculated the TPA cross sections using Eq. (1) for all samples, which are summarized in Table 2.

A relative comprehensive comparison between TPA cross sections in some standard reference dyes has been presented in [24]. In this reference, a value of 140 ± 20 GM for TPA cross section in Rhodamine B using a luminescence method has been reported, which is in agreement with our result (119 GM) within 15% error, but

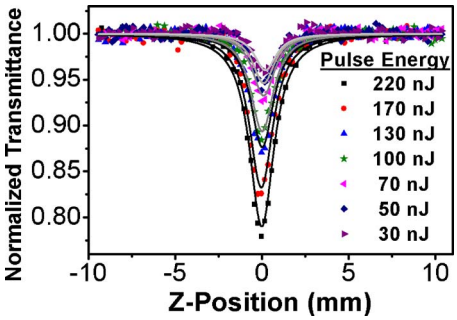

Fig. 6. (Color online) Z-scans for B3K performed with different pulse energies.

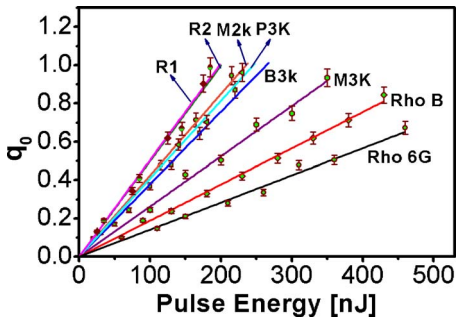

Fig. 7. (Color online) q_0 versus pulse energy for all samples.

a value of 50 GM has been reported in [30] using the Z-scan technique, which is smaller than our result by more than a factor of 2. This discrepancy can be explained as follows. In the literature, due to considering an ideal Gaussian beam without taking into account the beam quality factor, the peak intensity has been overestimated and thus has led to underestimating the TPA cross section. This discrepancy will be removed if a beam quality factor of 2 is considered, which represents the best case for a Ti:sapphire amplifier. This compatibility proves our argument that the beam quality factor must be taken into account. Therefore, we believe that our measurements are close to the actual values.

The compound M3P+ showed a very weak solubility in THF, and it was not possible to prepare a solution with a concentration of 1×10^{-2} M as for all other compounds. We prepared solutions with lower concentrations for M3P and M3P+ to compare their TPA cross sections.

We performed Z-scans for these two compounds with pulse energies up to 2 μJ at which the solvent started to nonlinearly absorb (a separate Z-scan was performed for the solvent to determine the energy at which the solvent starts to nonlinearly absorb). No TPA for M3P could be observed, whereas a hardly measurable TPA with a poor signal to noise ratio for M3P+ was observed. This indicates that the TPA cross section for M3P+ is larger than that for M3P.

No signal could be detected for H3K at energies up to 2 μJ, and a very weak signal was measured for O3K from which we estimated that its TPA cross section cannot be larger than 10 GM. Among the amino-based derivatives P3K had the highest value of 256 GM. The references R1 and R2 showed slightly higher values.

In some extent, linear and nonlinear absorption are linked. The TPA peak generally occurs at shorter wavelengths than twice the linear absorption peak [31]. Based on this link, we measured linear absorption spectra in order to estimate the TPA peak for all compounds [23]. The one-photon absorption (OPA) maxima and its corresponding extinction coefficient are presented in Table 2 for all samples. The OPA maxima for TPIs all are between 320 and 490 nm so that no OPA was observed for the wavelength longer than 580 nm. H3K has OPA maxima at 322 nm and no OPA at wavelengths larger than 380 nm, which implies that no TPA is possible for wavelengths larger than 760 nm as no TPA was observed for H3K at 800 nm. P3K and O3K have OPA maxima at 363 and 352 nm, respectively, and a hard measurable absorption at 400 nm. TPA cross sections for these two compounds were

Table 2. The TPA Cross Sections, the OPA Maxima, and the Extinction Coefficient for Reference Dyes in MeOH Solvent and Synthesized TPIs in THF as a Solvent at a Concentration of 1×10^{-2} M

Initiator	Rho 6G	Rho B	H3K	M3P+	O3K	M3P	M3K	B3K	P3K	M2K	R2	R1
TPA cross section (GM)[a]	89[b]	119[b]	—[c]	Not measurable[d]	<10	23	165	238	256	261	314	318
λ_{max}^{OPA} (nm)[e]	530	543	322	489	352	363	434	449	438	434	410	428
ε_{max}^{OPA} (M^{-1} cm^{-1}) [f]	116 000	106 000	25 000	44 000	32 000	57 000	53 000	65 000	50 000	48 000	57 000	65 000

[a]Measured in THF as solvent.
[b]Measured in MeOH.
[c]No signal observed.
[d]Poor solubility in THF.
[e]λ_{max}^{OPA} corresponds to the OPA maxima.
[f]ε_{max}^{OPA} corresponds to the decadic one-photon molar extinction coefficient (both λ_{max}^{OPA} and ε_{max}^{OPA} values were obtained by measuring in acetonitrile as solvent).

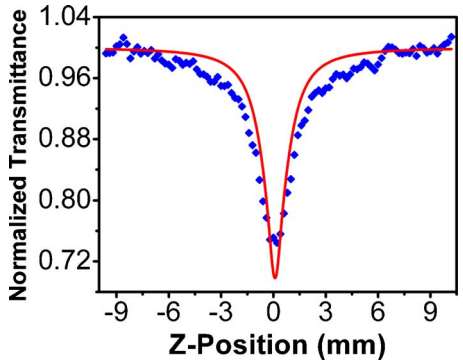

Fig. 8. (Color online) Z-scan for M2K with 330 nJ pulses. Solid line represents the fit curve assuming $z_R=0.7$ mm.

measured to be very small. All high absorptive compounds (M3K, B3K, P3K, M2K, R2, and R1) have a significant OPA at wavelengths between 350 and 450 nm, which shows that they could have a significant TPA at 800 nm. These results from OPA and TPA prove as mentioned above that, in some extent, linear and nonlinear absorptions are linked. However, it was not possible to measure the TPA spectra and determine the TPA maxima due to the lack of a wide range tunable laser source.

Among the new synthesized initiator materials, M2K showed a behavior different from the others. The Z-scan absorption curves are broader than expected as shown in Fig. 8. The theoretical curve using Eq. (2) does not fit appropriately to the experimental data with the Rayleigh length of $z_R=0.7$ mm as can be seen in Fig. 8. We believe that this is due to saturation, which is not taken into account in the fitting procedure, due to lack of an appropriate analytical formula. TPA saturation could be caused by various chemical reactions such as cis-trans isomerization processes upon exposure of the double bond. The TPA cross section obtained for M2K fits well to the value for analog compounds of M2K from the literature.

5. CONCLUSIONS

We have accurately measured TPA cross sections for a series of TPIs. Some of these synthesized TPIs such as B3K and P3K showed relatively high TPA cross sections (238 and 256 GM, respectively) and can be considered as good candidates for TPIP. It should be noted that this values may look small compared to some results found in the literature, but we emphasize that from the photochemistry side, our molecules are more related to the classical one-photon initiators that show very weak fluorescence. This has the advantage that all the absorbed energy is used to solidify and polymerize the material, and losses due to radiation are minimized. Therefore, we have shown that these molecules are very efficient TPA polymerization initiators by structuring test [23]. We comprehensively explained how one can measure the exact experimental parameters, i.e., the Rayleigh length and beam waist radius. An enhancement by a factor more than 2 was observed for TPA in all samples when we employed a syringe pump to flow materials which prevents materials from being destroyed during exposure (photo-degradation). A broadening in the Z-scan signal for M2K was observed which might be due to TPA saturation caused by cis-trans isomerization processes upon exposure of the double bond. A reduction in absorption in the vicinity of focus was observed when TPIs are exposed to ultrashort 25 fs pulses, which can be attributed to TPA saturation. It could also be concluded form our measurements for the TPA and OPA that the TPA can occur significantly at the wavelength twice the OPA maxima for molecular systems. Further experimental investigations for ultrashort pulses and further theoretical investigation to include TPA saturation are ongoing.

ACKNOWLEDGMENT

We acknowledge the Austrian Science Funds (FWF) for partly financial supporting this work in the framework of the Austrian Nano Initiative under contract No. N703.

REFERENCES

1. X. Deng, X. Zhang, Y. Wang, Y. Song, S. Liu, and C. Li, "Intensity threshold in the conversion from reverse saturable absorption to saturable absorption and its application in optical limiting," Opt. Commun. **168**, 207–212 (1999).
2. T. C. Lin, S. J. Chung, K. S. Kim, X. Wang, G. S. He, J. Swiatkiewicz, H. E. Pudavar, and P. N. Prasad, "Organics and polymers with high two-photon activities and their applications," Adv. Polym. Sci. **161**, 157–193 (2003).
3. J. Wang, M. Sheik-Bahae, A. A. Said, D. J. Hagan, and E. W. Van Stryland, "Time-resolved Z-scan measurements of optical nonlinearities," J. Opt. Soc. Am. B **11**, 1009–1017 (1994).
4. L. P. Liu, M. Zhou, Q. X. Dai, C. P. Pan, and L. Cai, "Three-dimensional micro-fabrication by femtosecond laser," Guangdian Gongcheng/Opto-Electronic Engineering **32**, 93–96 (2005).
5. C. C. Corredor, Z. L. Huang, and K. D. Belfield, "Two-photon 3D optical data storage via fluorescence modulation

of an efficient fluorene dye by a photochromic diarylethene," Adv. Mater. **18**, 2910–2914 (2006).
6. R. Houbertz, P. Declerck, S. Passinger, A. Ovsianikov, J. Serbin, and B. N. Chichkov, "Investigations on the generation of photonic crystals using two-photon polymerization (2PP) of inorganic-organic hybrid polymers with ultra-short laser pulses," Phys. Status Solidi A **204**, 3662–3675 (2007).
7. K. Ogawa and Y. Kobuke, "Recent advances in two-photon photodynamic therapy," Anti-Cancer Agents in Medical Chemistry **8**, 269–279 (2008).
8. S. Quentmeier, S. Denicke, and K. H. Gericke, "Two-color two-photon fluorescence laser scanning microscopy," J. Fluoresc. **19**, 1037–1043 (2009).
9. L. Antonov, K. Kamada, K. Ohta, and F. S. Kamounah, "A systematic femtosecond study on the two-photon absorbing D-π-A molecules-π-bridge nitrogen insertion and strength of the donor and acceptor groups," Phys. Chem. Chem. Phys. **5**, 1193–1197 (2003).
10. G. O. Clay, C. B. Schaffer, and D. Kleinfeld, "Large two-photon absorptivity of hemoglobin in the infrared range of 780–880 nm," J. Chem. Phys. **126**, 025102 (2007).
11. C. Xu and W. W. Webb, "Measurement of two-photon excitation cross sections of molecular fluorophores with data from 690 to 1050 nm," J. Opt. Soc. Am. B **13**, 481–491 (1996).
12. J. D. Bhawalkar, G. S. He, and P. N. Prasad, "Nonlinear multiphoton processes in organic and polymeric materials," Rep. Prog. Phys. **59**, 1041–1070 (1996).
13. Q. Yang, J. Seo, S. Creekmore, G. Tan, H. Brown, S. M. Ma, L. Creekmore, A. Jackson, T. Skyles, B. Tabibi, H. Wang, S. Jung, and M. Namkung, "Z-scan and four-wave mixing characterization of semiconductor cadmium chalcogenide nanomaterials," J. Phys.: Conf. Ser. **38**, 144–147 (2006).
14. A. Ajami, M. S. Rafique, N. Pucher, S. Bashir, W. Husinsky, R. Liska, R. Inführ, H. Lichtenegger, J. Stampfl, and St. Lüftenegger, "Z-scan measurements of two-photon absorption for ultrashort laser radiation," Proc. SPIE **7027**, 70271H (2008).
15. M. Sheik-Bahae, A. A. Said, T. H. Wei, D. J. Hagan, E. W. Van Stryland, and M. J. Soileau, "Sensitive n2 measurements using a single beam," NIST Special Publication No. 801, (NIST, 1990), pp. 126–135.
16. M. Sheik-Bahae, A. A. Said, T.-H. Wei, D. J. Hagan, and E. W. Van Stryland, "Sensitive measurement of optical nonlinearities using a single beam," IEEE J. Quantum Electron. **26**, 760–769 (1990).
17. H. Ma and C. B. De Araujo, "Two-color Z-scan technique with enhanced sensitivity," Appl. Phys. Lett. **66**, 1581–1583 (1995).
18. T. Xia, D. I. Hagan, M. Sheik-Bahae, and E. W. Van Stryland, "Eclipsing Z-scan measurement of $\lambda/10^4$ wave-front distortion," Opt. Lett. **19**, 317–319 (1994).
19. D. V. Petrov, A. S. L. Gomes, and C. B. De Araujo, "Reflection Z-scan technique for measurements of optical properties of surfaces," Appl. Phys. Lett. **65**, 1067–1069 (1994).
20. S. L. Guo, J. Yan, L. Xu, B. Gu, X. Z. Fan, H. T. Wang, and N. B. Ming, "Second Z-scan in materials with nonlinear refraction and nonlinear absorption," J. Opt. A, Pure Appl. Opt. **4**, 504–508 (2002).
21. A. I. Ryasnyansky and B. Palpant, "Theoretical investigation of the off-axis z-scan technique for nonlinear optical refraction measurement," Appl. Opt. **45**, 2773–2776 (2006).
22. J. M. Menard, M. Betz, I. Sigal, and H. M. Van Driel, "Single-beam differential z-scan technique," Appl. Opt. **46**, 2119–2122 (2007).
23. N. Pucher, A. Rosspeintner, V. Satzinger, V. Schmidt, G. Gescheidt, J. Stampfl, and R. Liska, "Structure-activity relationship in D-π-a-π-D-based photoinitiators for the two-photon-induced photopolymerization process," Macromolecules **42**, 6519–6528 (2009).
24. N. S. Makarov, M. Drobizhev, and A. Rebane, "Two-photon absorption standards in the 550-1600 nm excitation wavelength range," Opt. Express **16**, 4029–4047 (2008).
25. B. A. Reinhardt, "Two-photon technology: New materials and evolving applications," Photonics Sci. News **4**, 21–33 (1999).
26. A. Rosspeintner, M. Griesser, N. Pucher, K. Iskra, R. Liska, and G. Gescheidt, "Toward the photoinduced reactivity of 1,5-diphenylpenta-1,4-diyn-3-one (DPD): Real-time investigations by Magnetic resonance," Macromolecules **42**, 8034–8038 (2009).
27. T. F. Johnston, Jr., "Beam propagation (M^2) measurement made as easy as it gets: The four-cuts method," Appl. Opt. **37**, 4840–4850 (1998).
28. K. D. Belfield, K. J. Schafer, Y. Liu, J. Liu, X. Ren, and E. W. Van Stryland, "Multiphoton-absorbing organic materials for microfabrication, emerging optical applications and non-destructive three-dimensional imaging," J. Phys. Org. Chem. **13**, 837–849 (2000).
29. L. Antonov, K. Kamada, and K. Ohta, "Estimation of two-photon absorption characteristics by a global fitting procedure," Appl. Spectrosc. **56**, 1508–1511 (2002).
30. R. Sailaja, P. B. Bisht, C. P. Singh, K. S. Bindra, and S. M. Oak, "Influence of multiphoton events in measurement of two-photon absorption cross-sections and optical nonlinear parameters under femtosecond pumping," Opt. Commun. **277**, 433–439 (2007).
31. U. Gubler and C. Bosshard, "Molecular design for third-order nonlinear optics," Adv. Polym. Sci. **158**, 123–191 (2002).